

Potential Mechanism of Ziyin Tongluo Formula in the Treatment of Postmenopausal Osteoporosis based on Network Pharmacology and Ovariectomized Rat Model

Chen Rongbin

Guangzhou University of Chinese Medicine

Yang Yingdong

Guangzhou University of Chinese Medicine

Sun Kai

Guangzhou University of Chinese Medicine

Liu Shan

Guangzhou University of Chinese Medicine

Guo Wei

Guangzhou University of Traditional Chinese Medicine First Affiliated Hospital

Zhang Jinxin

Guangdong Provincial Hospital of Traditional Chinese Medicine ZHUHAI BRANCH

Li Yong (✉ yygctm@163.com)

Guangdong Province Hospital of Traditional Chinese Medicine ZHUHAI BRANCH

<https://orcid.org/0000-0003-4257-032X>

Research

Keywords: Postmenopausal osteoporosis, Ziyin Tongluo Formula, Traditional Chinese medicine, Ovariectomy, Network pharmacology, Molecular docking

Posted Date: June 29th, 2021

DOI: <https://doi.org/10.21203/rs.3.rs-649560/v1>

License:   This work is licensed under a Creative Commons Attribution 4.0 International License.

[Read Full License](#)

Potential Mechanism of Ziyin Tongluo Formula in the Treatment of Postmenopausal Osteoporosis: Based on Network Pharmacology and ovariectomized rat model

Rong-Bin Chen^{1,2} Ying-Dong Yang¹ Kai Sun¹ Shan Liu³ Wei Guo¹ Jin-Xin Zhang² Yong Li^{2*}

*Correspondence: lyzhuhai666@126.com

¹ The Second Clinical Medicine College, Guangzhou University of Chinese Medicine, Guangzhou 510006, China.

Full list of author information is available at the end of the article.

Abstract

Background: Amending from ancient classic, Ziyin Tongluo Formula (ZYTLF) has been prescribed to treat Postmenopausal osteoporosis (PMOP) for decades and obtained beneficial effect. However, the possible mechanisms of it are still unknown.

Methods: Ovariectomized rat model were established to validate the therapeutic effect of ZYTLF on PMOP by Micro-CT bone analysis and pathological observation. Subsequently, active ingredients of ZYTLF and corresponding putative targets were identified by online databases. Overlapping genes were obtained by mining genes associated with PMOP and then overlapping them with the putative targets. Key genes were selected from the multiple constructed and analyzed networks. GO and KEGG pathway enrichment analysis were performed by importing the key genes to the DAVID database. Moreover, validation of the binding association between key targets and their corresponding active compounds were accomplished by AutoDock Tools and other softwares. Lastly, Enzyme linked immunosorbent assay (Elisa) detection and Western blot analysis were utilized to further explore the possible mechanism of ZYTLF on PMOP.

Results: With 129 target genes interacting with PMOP, 92 active compounds of ZYTLF corresponded to 243 targets, and 50 key genes were chosen. Network analysis revealed the top 10 active ingredients, such as quercetin, kaempferol and the top 50 key genes, such as ER α , p38 MAPK, p-AKT, TGF- β 1.

Enrichment analysis uncovered multiple signaling pathways, including estrogen signaling pathway, TNF signaling pathway, PI3K–Akt signaling pathway, MAPK signaling pathway. Furthermore, our finding of the foremost active compounds were tightly bound to the core proteins was verified by molecular docking analysis. We confirmed that the prescription of ZYTLF could ameliorate the OVX-induced bone loss, suppress the osteoclast activity and boost osteoblastg ability through experimental studies.

Conclusion: The potential mechanisms and therapeutic effects of ZYTLF against PMOP may be ascribed to inhabit osteoclast activity, boost osteoblast activity and enhance the expression of ER α .

Keywords: Postmenopausal osteoporosis, Ziyin Tongluo Formula, Traditional Chinese medicine, Ovariectomy, Network pharmacology, Molecular docking

Background

Postmenopausal osteoporosis (PMOP) is regarded as a severe chronic metabolic bone disease. There are increasing number of postmenopausal women around the world suffering from increased fragility and fracture susceptibility because of decreased ovarian function and estrogen levels every year. At this stage of life, the bone resorption is faster than the bone building. Therefore, the incidence rate of osteoporosis steps up in the population of women of menopausal age with plummeted estrogen levels. Factors such as age, gender, genetics, reproductive status, calcium:phosphorus ratios, and exercise have certain impacts on bone strength. Bone strength is consisted of bone mineral density(BMD) and bone quality. BMD is detected with dual energy absorptiometry (DXA) and declined by 30-40% at the age of 70s. However, there are many elderly patients who present with vertebral fractures but have bone density within the normal range in the ward. Bone quality deterioration is also closely associated with the fracture. [1-2]. With the characteristics of low bone mass and bone microstructure destruction in histological morphology, PMOP is associated with fractures due to decreased bone strength. As a common complication, osteoporotic fracture is one of the main culprits that leads to disability and death in postmenopausal women. The incidence of osteoporotic fractures is 40.9% in Chinese women at the age of 50s and it is distinctly higher than that of 8.7% in Chinese men, posing a huge burden on both individuals and society for its enormous cost and high risk of subsequent complications, such as pneumonia [3-4].

Hormone replacement therapy (HRT) in postmenopausal women enhances their estrogen levels and effectively reduces bone resorption, but its safety is still controversial [5]. A meta analysis, including twenty-seven randomized controlled trials, indicates that alendronate had better efficacy on improving BMD and lower risk of adverse effect than raloxifene [6]. With high efficacy of inhibiting bone resorption, bisphosphonates is perceived as the first-line therapy for PMOP; however, its unclear short-and long-term safety also arouse public concerns. Therefore, limited options of clinically available treatments for PMOP highlights the urging demand to develop alternative agents with better efficacy and safety. As one of the major modalities in complementary and alternative medicine, Traditional Chinese Medicine (TCM) has a long history in treating osteoporosis. It has low side effects, rich resources and remarkable efficacy. According to modern pharmacological experiments, various traditional Chinese herbs contain active ingredients against osteoporosis, and formulas of traditional Chinese herbs can treat osteoporosis in a more effective way than a single herb does[7-8]. TCM, as an optional therapy, has got increasingly more attention.

Ziyin Tongluo Formula (ZYTLF) is amended from an ancient classic, based on the constitution of person in the lingnan (south of the five ridges), China. As a folk remedy, ZYTLF contains Radix Rehmanniae Praeparatae, Ophiopogon japonicus, Achyranthes bidentata, Fructus Ligustri Lucidi, Radix Angelicae Sinensis, Radix Paeoniae Alba, Loranthus parasiticus, Caulis Spatholobi, Zaoocys, Scolopendra, Radix Astragali, Saposhnikovia Radix, Rhizoma Atractylodis Macrocephalae, Radix Glycyrrhizae Preparata. ZYTLF has been perscribed for decades to prevent and treat postmenopausal osteoporosis, effectively alleviating patients' clinical symptoms and increasing their bone density[9]. Nevertheless, the Pharmacological mechanism of ZYTLF on PMOP is completely unclear.

Therefore, in this work, network pharmacology was applied to mine the key ingredients, targets and signaling pathways of ZYTLF against on PMOP. Moreover, molecular docking simulations were utilized to validate the stability of key proteins and corresponding compounds by detecting binding affinity. Furthermore, ovariectomized rat models were established to confirmed the therapeutic effect of ZYTLF on PMOP and elucidate its preliminary mechanisms. (Figure1)

Methods

ZYTLF preparation

The name and formula ratios of fourth herds of ZYTLF are shown in Table1. The qualified granule ingredients of

ZYTFL were purchased from Guangdong Province Hospital of Traditional Chinese Medicine Zhuhai Branch. A 60 g of ZYTFL granules components were blended with 40 ml ultrapure water and make it to a ultimate density of 3 g/mL.

Generation of OVX animal models

Experimental animal ethics panel of the Guangdong Provincial Hospital of Traditional Chinese Medicine (License NO.2019044) ethically approved the animal experiments and they were performed in China Academy of Chinese Medical Sciences Guangdong Branch (License NO.00228297). Sixty three-month-old female Sprague-Dawley (SD) rats, weighting 200-230g, were purchased from the Laboratory Animal Center of Southern Medical University (License No.44002100022874) and were allowed to acclimatize for one week before free access to food and space. All animal procedures complied with international ethical guidelines and the National Institutes of Health Guide concerning the Care and Use of Laboratory Animals. We tried our best to attenuate the number and suffering of the animals.

The rats received either sham operation (SHAM, n=10) or bilateral ovariectomy (OVX, n=40). All operations were performed with the application of anesthesia methods and sterile techniques as well as postoperative anti-infection and analgesia. Three months after ovariectomy, if the BMD of the rats were decreased significantly, the OVX animal model was judged to be successful.

ZYTFL administration

Five groups of qualified rats were randomly divided (OVX, OVX+ZYTFL low dose, OVX+ZYTFL mid dose, OVX+ZYTFL high dose, OVX+WM (Western Medicine)). The rats in the SHAM group and OVX group were gavaged by distilled water, the OVX+ZYTFL Low / Middle / High dose group were administrated $1.34 \text{ g} \cdot \text{kg}^{-1}$, $2.68 \text{ g} \cdot \text{kg}^{-1}$, $4.02 \text{ g} \cdot \text{kg}^{-1}$ per day respectively, and the OVX+WM group were treated with alendronate 10.51 mg/kg per week and calcitriol $0.075 \mu \text{g/kg}$ per day for 12 weeks. Rat intake dose was modified according to half, one or two times of the clinical human dose. The conversion obeys the Human-Rat Equivalent Dose Conversion Principle.

After the last 24 hours of medicinal treatment, overdose of anesthesia was used to euthanize the animals. The rats were anesthetized after three months. Blood samples from the abdominal aorta were first centrifuged at 4000 rpm for 10 minutes. Then the serum was removed and the samples were stored at -20°C . Lumbar vertebra body and bilateral femur and tibia were also removed as samples.

Enzyme linked immunosorbent assay (Elisa) detection

The contents of estradiol (E2), alkaline phosphatase (ALP), procollagen I N-terminal propeptide (PINP), tartrate-resistant acid phosphatase (TRACP), type I collagen cross-linked Amino Terminal Peptide (NTX), type I collagen cross-linked carboxyl Terminal Peptide (CTX-1), calcium (Ca), phosphorus (P) in rat serum samples were confirmed by commercial ELISA kits based on manufacturer's instructions. The ELISA kits were purchased from Nanjing Jiancheng Bioengineering Institute, NanJin,China.

Micro-CT bone analysis

Bone structural and mineral changes in rats were evaluated by micro-computed tomography (micro-CT) technique. A micro-CT imaging system (Bruker skyscan 1172, Belgium) was applied to perform the CT scan and trabecular morphometric analysis under the guidance of manufacturer's application notes. A spatial resolution of $9\ \mu\text{m}$ (X-ray source 80 kV, $384\ \mu\text{A}$; 1 mm filter applied) was used to scan right femur samples. After that, CT images were reestablished by in-built software CT-vox and CTAn respectively. With recommended order set, CTAn selected the trabecular region of interest in an unbiased batch. The aim of performing trabecular analysis was to quantify morphometric calculations and BMD.

The measured direct trabecular metric parameters of right femur were as follows: trabecular thickness (Tb.Th), bone volumetric fraction (BV/TV), trabecular number (Tb.N) as well as trabecular separation (Tb.Sp). Calculations of directly measured non-metric parameters were performed as well, including the trabecular bone pattern factor (Tb.Pf), an inverse assessment of trabecular connectivity and the structural model index (SMI), an estimate of the prevalence of plate-like or rod-like trabecular.

Pathological observation

The left tibial tissue was acquired and fixed in 4% paraformaldehyde for 24 h and then decalcified for 2 weeks in 10% EDTA buffer (pH 7.0). The samples were dehydrated, embedded in paraffin and cut into slices (about $4\ \mu\text{m}$ thick). Slices were processed with tartrate-resistant acid phosphatase (TRAP)-staining and alkaline phosphatase (ALP)-staining respectively, aiming to detect the number of osteoclasts and osteoblasts. The sections were visualized by using an optical microscope (Olympus, Shanghai, China) and photographed. The cytoplasm of osteoclasts is wine-red and the cytoplasm of osteoblasts shows grayish-black granules after ALP+TRACP staining.

Network Pharmacology Analysis

Database preparation

Fourteen herbs of ZYTTF were in sequence inputted into the Traditional Chinese Medicine Systems

Pharmacology Database and Analysis Platform (TCMSP <http://tcmospw.com/tcmosp.php>) [10], BAT-MAN TCM (<http://bionet.ncpsb.org/batman-tcm/>) [11] and Traditional Chinese Medicine Information Database (TCMID, <http://www.megabionet.org/tcmid/>) [12] to find certain or potential corresponding compounds. Oral bioavailability (OB) and drug-likeness (DL) were set as standards for screening active compounds. Compounds that were considered as biologically active ingredients shall meet the standard of $OB \geq 30\%$ and $DL \geq 0.18$. Since *Radix Glycyrrhizae Preparata* is of less importance in this prescription, greater bias was avoided by setting the standard as $OB \geq 60\%$ and $DL \geq 0.36$. The targets of ZYTFL were collected by TCMSP analysis platform and then were transferred to standard protein name in Uniprot database (<https://www.Uniprot.org>), setting organisms as Human [13].

"Postmenopausal" and "Osteoporosis" were the key words to gather PMOP connected genes from the three following on-line databases: Genecards (<http://www.genecards.org>) [14], OMIM (<http://omim.org/>) [15], and DisGenet (<https://www.disgenet.org/>) [16]. Overlapping target genes that could be potential targets for ZYTFL against PMOP were later obtained from ZYTFL target genes and PMOP-related genes.

Network Analysis

A "herb-compound-overlapping gene" network model was built by importing the overlapping target genes, their corresponding active components and herbs into Cytoscape 3.7.1 [17]. CytoNCA plug-in [18] was applied to perform network topology analysis. Key nodes in the network were screened in light of the Degree Centrality (DC) and Between Centrality (BC). The higher the node's degree value was, the more important it was in the network.

Construction of overlapping proteins' protein-protein interaction (PPI) network was completed through setting the condition of data analysis mode as "Multiple proteins", the type as "Homo sapiens" (human), and the minimum mutual threshold as "high confidence (0.700)" by The STRING database (<http://string-db.org/>, ver.11.0) [19]. The other parameters were unaltered. The data of PPI network was obtained and then inputted into Cytoscape 3.7.1. Core genes were screened out by network analysis conducted with The MCC algorithm in the CytoHubba plug-in.

The Database Visualization and Integrated Discovery system (DAVID, <https://david.ncifcrf.gov/>) was utilized to conduct enrichment analysis of Gene Ontology (GO, <http://www.geneontology.org/>) and Kyoto Encyclopedia of Genes and Genomes (KEGG, <http://www.genome.jp/kegg/>) [20-21], setting race "Homo sapiens". Advanced bubble diagrams were drawn by R software.

Molecular docking simulation

The binding efficiency of the overlapping proteins and major active components in ZYTLFT were evaluated by computer simulation docking technology. The SDF structure of top 10 core compounds were collected in the network from the PubChem database (<https://pubchem.ncbi.nlm.nih.gov/>). Procession and transformation of the 2D structure into PDB format were accomplished by PyMOL, and they were saved in PDBQT format as docking ligands. Concurrently, the collection of all the crystal structures of the key proteins from the RCSB protein data bank (PDB, <http://www.pdb.org/>) and the selection of those with distinctive ligands and comparatively higher resolution were done. AutoDock Tools was used to take away the water molecules, isolate proteins and reserve them as receptors. The receptors and ligands were processed with PyMOL and Auto Dock and then docked through Vina.

Western blot analysis

Radioimmunoprecipitation assay (RIPA) buffer that contained Halt Phosphatase Inhibitor Cocktail (Thermo Scientific, USA) were ground with right tibia samples, which were corrected based on the results of the bicinchoninic acid assay (BCA). 10%SDS-PAGE separated 30 μ g protein. Then they were transferred to polyvinylidene fluoride (PVDF) membranes (Millipore, USA). In order to maximize the protein loading, membranes were air-dried and reactivated in methyl alcohol. According to the purpose of the experiment, they were blocked with 5% nonfat milk powder at room temperature, and incubated with primary antibody, including ER α (1:1,000, Abcam, Cambridge, UN), TGF- β 1 (1:1,000, Cambridge, UN), p38 MAPK (1:2,000, Cambridge, UN), p-AKT (1:1,000, Cambridge, UN), and GAPDH (1:1,000, Cambridge, UN) at 4 $^{\circ}$ C overnight. The nitrocellulose membranes were washed 3 times with PBST and incubated with goat anti-rabbit IgG antibody (1:15000, Zs-BIO, Shanghai, China) at room temperature for 2h. After these procedures, they were rinsed 3 times and scanned for optimal density value of the target protein unit by improved Journal Pre-proof chemiluminescence analysis (Thermo, MA, USA).

Statistical Analysis

All statistical analyses of this paper were performed by GraphPad Prism 8.0.2 (San Diego, USA). The data were represented by means \pm standard deviation (SD). Statistical analyses with various comparisons were conducted with one-way ANOVA analysis, followed by Dunnett's post hoc test to confirm the differences between test groups and nominated control group, with the significance level at $P < 0.05$.

Results

Effects of ZYTLF on serum indicators in OVX rat

By ELISA detection, the rats in OVX group showed lower level of E2 ($p < 0.05$, Figure 2a), ALP ($p < 0.01$, Figure 2b), PINP ($p < 0.01$, Figure 2c) and higher level of TRACP ($p < 0.05$, Figure 2d), CTX-1 ($p < 0.05$, Figure 2f) than sham group. The results indicates ZYTLF not significantly change the levels of E2, however, ZYTLF significantly increased the level of ALP ($p < 0.05$) and PINP ($p < 0.05$), and inhibited the level of TRACP ($p < 0.05$), NTX ($p < 0.05$, Figure 2e) and CTX-1 ($p < 0.01$) in comparison to the OVX group. There is no significant different in the level of Ca between ZYTLF treatment group and OVX group ($p < 0.05$, Figure 2g).

Micro-CT evaluation

As shown in Figure 3, compared with the sham group, the BMD in the OVX group considerably decreased ($P < 0.05$). 1.34g/kg ZYTLF not significantly elevated the BMD, whereas 2.68g/kg ($p < 0.05$), 4.02g/kg ($p < 0.05$) ZYTLF and western medicine significantly elevated BMD compared with those in the untreated OVX rats.

In the Figure 2b-2g, structure model index (SMI) and trabecular bone pattern factor (Tb.Pf) were noticeably more prominent in the OVX group, while bone volume fraction (BV/TV) and trabecular number (Tb.N) were markedly lower than those parameters in the SHAM group. In the 2.68g/kg, 4.02g/kg ZYTLF and western medicine treatment groups, Tb.N were significantly increased and compared with those of the OVX group, SMI observably reduced. Nevertheless, on BV/TV, Tb.N and Tb.Pf from ovariectomy, 1.34g/kg ZYTLF group represented weaker rescue effect in comparison with SHAM group.

The micro-CT plain scan (sagittal and transverse) of the distal femoral bone were shown in Figure 4. Though from all transverse and sagittal images, there's no significant loss of cortical bone, trabecular bone had less spreading, thinning structure and dilated interval space in comparison with SHAM group. Consistent with BMD results, OVX rats reduced remarkably in trabecula. 2.68g/kg, 4.02g/kg ZYTLF and western medicine markedly prevented bone mineral loss in trabecular bone from OVX.

Pathological observation of the tibia

Figure 5 shows histological micrographs of the rat tibias. Osteoclast numbers, osteoblast numbers and morphology were normal in the tibia of the sham ground. The number of osteoclast increased in the OVX ground but the number of osteoblast reduced. In the contrast, the number of osteoclast and osteoblast in the OVX+ZYTLF grounds were normal as the level of the sham ground.

Active ingredients of ZYTLF and overlapping genes

A total of 1,738 compounds were obtained from TSMSP platform, BAT-MAN TCM and TCMID database, among which 92 met the requirement were regarded as active components. Additional file 1:Table S1 displayed the elaborated data of active components of ZYTTF. There were totally 242 corresponding target genes for these active components.

After removing duplication, totally 1113 PMOP related genes were collected From Genecard, Disgenet and OMIM databases. Compared target genes of ZYTTF with PMOP-related genes, 129 overlapping target genes were collected altogether. (Figure.6a). Details about ZYTTF-genes, PMOP-genes, and ZYTTF-PMOP overlapping target genes are presented in Additional file 2:Table S2.

Network analysis

A network of "herb-compound-overlapping gene" was established (Figure.6b). Additional file 3:Table S3 showed the detailed information of the network with 231 nodes and 1,072 edges. According to topology analysis of the network, active ingredients such as quercetin, kaempferol, luteolin, scutellarein, and formononetin had higher degrees, which also played a vital part within the network.

After setting the relevant parameters, intersecting genes were imported into the STRING database to build a PPI network. The network represented the relevant details of the genes and the interaction association. (Figure.6c). Then the PPI network information was visually handled and analyzed by Cytoscape 3.7.1 software. The selection of top 50 key genes were based on the MCC algorithm of the CytoHubba plug-in. (Figure.6d).

GO and KEGG enrichment analysis

Performance of GO enrichment and KEGG pathway enrichment analysis on 50 core genes and extraction of significant enrichment results (FDR < 0.05) was done by DAVID database. Totally, 62 GO-BP terms, 6 GO-CC terms, 11 GO-MF terms and 59 terms on the KEEG pathway were obtained. The enrichment results showed that positive transcriptional regulation signals of RNA polymerase II promoter, negative regulation of apoptosis, positive regulation of transcription using DNA as a template, aging, positive regulation of gene expression, etc. Main cell components such as nucleus, cytoplasm and extracellular space were the major components of biological processes. Major regulated molecular functions were binding of enzyme , transcription factor and protein binding. (Figure.7a-c). Fifteen signal pathways associated with PMOP were markedly enriched KEGG analysis. Figure.7d) altogether, including estrogen signaling pathway, TNF signaling pathway, PI3K-Akt signaling pathway, MAPK signaling pathway. Additional file 4:Table S4 elucidated the results and details on the GO terms and pathways .

The core compounds in ZYTLF are docked with key proteins

Whether the top 10 compounds were essential in regulating the 50 key proteins was verified by molecular docking simulation. A stable structure will be formed when the ligand binds to one or more amino acid residues in the active site (also called active pocket) of the receptor and takes part in the process such as conformation change and energy complementation to combine with the receptor. This research illustrated that the top 10 compounds had sturdy association with 50 core proteins, such as AKT1 (PDB id: 6npz), MAPK14(PDB id:6sfo), ER α (PDB id: 4pxm), TNF (PDB id:3m2w), TGF- β 1 (PDB id:6om2) and PTGS2 (PDB id:5f19). These compounds are of great importance based on the result of network pharmacology (Table 2). The ligands and receptors are considered to be able to form stable compounds when the binding energy is less than -5 kcal/mol. Details of the binding energies of the different compounds are shown in Additional file 5:Table S5.

ZYTLF modulated the expression of ER α , p38 MAPK , p-AKT, TGF- β 1, OPG , RANKL and OPG/RANKL ratio.

To determine the mechanism in ZYTLF treated PMOP, expression of six key proteins in bone tissues after ZYTLF treatment were examined (Figure 8). ER α , TGF- β 1, p38 MAPK, p-AKT, OPG protein level in bone tissue was dramatically elevated by ZYTLF treatment in contrast to OVX group in a dose-dependent manner. Moreover, RANKL protein level was suppressed markedly in ZYTLF groups.

Discussion

In ovariectomized rat model, a sudden and dramatic decrease in the estrogen production follow the arrest of ovarian function. Estrogen deficiency boosts bone resorption from stimulating osteoclast formation and lifespan. In this condition, osteoblast formation also is stimulated, but this increased bone turnover shifts the bone homeostasis toward bone resorption, resulting in rapid trabecular bone loss and an increased risk of skeletal fracture.

In this study, we found that ZYTLF and alendronate treatment inhibited the bone loss in rats induced by OVX. The BMD of OVX rats was improved by middle and high dose ZYTLF that was similar to the change showed in alendronate treatment. Moreover, ZYTLF showed similar effect with alendronate on trabecular microstructure indexes. Bone volume fraction (BV/TV) and trabecular number (Tb.N) , trabecular thickness (Tb.Th), and trabecular separation (Tb.Sp), trabecular bone pattern factor (Tb.Pf), SMI index. The results indicated that ZYTLF could mitigate microstructure degeneration in OVX rats and preserve more thick,

interwoven and plate-like trabecular bones. These observations demonstrate ZYTFLF ameliorates trabecular bone resorption in OVX induced rat model with high turnover bone metabolism. Furthermore, our bone pathological analysis with ALP+TRACP staining and detection of bone metabolic markers confirmed that ZYTFLF could ameliorate the bone phenotype of OVX rats, reduce the osteoclast formation and increase osteoblast differentiation. Many TCM therapy has effect on promoting OB generation and inhibiting OC differentiation, as ZYTFLF does. However, ZYTFLF's effect on osteoclastogenesis and osteoblastogenesis is still uncertain.

Preliminary determination of the pharmacological compounds and complex molecular mechanisms of ZYTFLF on PMOP were done by molecular docking technology and network pharmacology. Network pharmacology is a systematic approach employed to learn the complexities among compounds, targets, diseases and biosystems. It coincides with the holistic and systemic views of TCM theory[22]. Currently, the pharmacological action, safety and sophisticated molecular mechanisms of TCM are mostly investigated by network pharmacology. The results from network pharmacology were further verified by the computer simulation docking technology through evaluation of the binding efficiency of the overlapping proteins and main active components in ZYTFLF. Through the screening of active ingredients and analysis of compound-target network, quercetin and kaempferol were considered as the main compounds of ZYTFLF exerting pharmacological effect. With the highest degree value in the network, Quercetin is a representative flavonoid compound. It has various pharmacological effects, such as anti-infection, anti-cancer, anti free-radical, and cardiovascular protection[23-26]. Li found that possibly by up-regulating gene expression of ALP and inhibiting signaling pathways of JNK, ERK, and p38 MAPK, quercetin could ameliorate osteoporosis symptoms in ovariectomized rats[27]. Kaempferol has also been proved of protecting bones on ovariectomized rats [28], possibly through estrogen receptor, MAPK, NF- κ B and other signaling pathways [29].

The data revealed 50 putative targets were involved in pharmacological action of ZYTFLF on PMOP, in which ER α , p38 MAPK , p-AKT, TGF- β 1 were considered as hub proteins. Moreover, 15 KEGG pathways were observably enriched by KEGG analysis, including estrogen signaling pathway, TNF signaling pathway, PI3K-AKT signaling pathway, MAPK signaling pathway, osteoclast differentiation which were closely bound with the development and progression of PMOP. Estrogen bound with the estrogen receptor in osteoblasts and osteoclasts to act on the OPG/RANK/RANKL signaling pathway, which further propelled secretion of OPG, down-regulated the expression of RANKL, and inhibited the formation of osteoclasts[30]. It is widely

acknowledged that the falling levels of estrogen in postmenopausal women can stimulate the immune system to supply an oversized amount of osteoclastogenic factors, which later activates related signaling pathways and further aggravates bone loss[31]. According to in-vitro experiments, through NF- κ B and PI3K/Akt signaling pathways, TNF- α and RANKL concertedly improve bone resorption of osteoclasts [32].

It is generally considered that estrogen deficiency is the major cause of the occurrence and development of PMOP, so the current research mainly focuses on how to elevated estrogen level. Interestingly, this research found that ZYTFLF did not significantly boosted estrogen levels, but reduced bone loss to normal bone homeostasis. Through western-blot analysis, we found that ZYTFLF treatment increased the expression of ER α protein in bone sample. ER α has been proved to plays a critical role in bone metabolism. The expression of ER α in bone tissues is estrogen-dependent, and the transcription and translation of ER α are inhibited after the level of estrogen is reduced[33]. On the other hand, after the combination of estrogen and estrogen receptor, it could also regulate the expression of various target genes through the estrogen signaling pathway, so that downstream PI3K/Akt, MAPK, WNT and other signaling pathways could be activated to enhance the proliferation and differentiation of osteoblasts [34-35]. Our study suggested that excessive expression of ER α may activated the downstream proteins, including p-AKT, p38-MAPK, TGF- β 1, OPG. By increasing estrogen receptor expression, rather than raising estrogen levels, this may be a new idea of treatment for PMOP in the future.

There are also several limitations about this study. First, the screened active components by network pharmacology are not identical to the actual components in blood. Second, ZYTFLF need to be proved to have little effect on expression of ER in uterus and mammary gland.

Conclusion

In summary, our findings illuminated that ZYTFLF ameliorate the OVX-induced bone loss, suppress the osteoclast activity and boost osteoblastg ability. Moreover, the key compounds and target proteins were mined, such as quercetin, kaempferol and ER α , p38 MAPK , p-AKT, TGF- β 1, which were considered as the materials of ZYTFLF treated PMOP. In addition, multiple signaling pathways, including estrogen, MAPK, PI3K/Akt and OPG/RANK/RANKL signaling pathways, involved the treatment mechanisms. Consequently, this study provides postmenopausal osteoporosis with experimental evidence of ZYTFLF as a rational treatment, and preliminarily indicated its mechanism.

Appendix

Acknowledgements

Not applicable

Funding

This study was supported by grants from Traditional Chinese Medicine Bureau Of Guangdong Province of China for Arranged Project of Experiential prescription (No. 20194010) and Scientific research project of Traditional Chinese Medicine Bureau Of Guangdong Province of China (No. 20212213). Funder provided financial support for the study.

Abbreviations

PMOP: postmenopausal osteoporosis; ZYTLF: Ziyin Tongluo Formula; TCMSA: traditional Chinese medicine system pharmacology analysis platform; GO: Gene Ontology; KEGG: Kyoto Encyclopedia of Genes and Genomes; BP: biological processes; CC: cellular components; MF: molecular functions; OB: oral bioavailability; DL: drug-likeness; ADME: absorption, distribution, metabolism, excretion; IL-6: Interleukin 6; TNF: Tumor necrosis factor.

Availability of data and materials

The datasets used and analyzed during the current study are available from the corresponding author on reasonable request.

Ethics approval and consent to participate

Not applicable

Competing interests

The authors declare that they have no competing interests.

Consent for publication

Not applicable

Authors' contributions

YL and RBC conceived and designed the study. RBC and YDY drafted the manuscript. JXZ and SL collected the data. YDY, KS and WG performed the data analysis. KS, SL, and WG provided advice during the study and manuscript preparation. All authors read and approved the final manuscript.

Author's information

Rong-Bin Chen (469843897@qq.com), Ying-Dong Yang (125159770@qq.com), Kai Sun (961220881@qq.com), Shan Liu (liushan@gzucm.edu.cn), Wei Guo (844608579@qq.com), Jin-Xin Zhang (352339532@qq.com), Yong Li (lyzhuhai666@126.com)

Author details

¹The Second Clinical Medicine College, Guangzhou University of Chinese Medicine, Guangzhou 510006, China. ²GuangDong Province Hospital Of Traditional Chinese Medicine ZHUHAI BRANCH, Zhuhai 519015, China. ³The Research Center of Basic Integrative Medicine, Guangzhou University of Chinese Medicine, Guangzhou 510006, China.

References

1. Fujiwara S. Epidemiology of respiratory diseases and osteoporosis. *Clin Calcium* 2016;26 (10):1387-1392. Japanese. PMID: 27666684.
2. Eastell R, O'Neill TW, Hofbauer LC, Langdahl B, Reid IR, Gold DT, Cummings SR. Postmenopausal osteoporosis. *NAT REV DIS PRIMERS* 2016;2(1). <https://doi.org/10.1038/nrdp.2016.69>.
3. Lei Si, Tania M. Winzenberg, Mingsheng Chen, Qicheng Jiang, Andrew J. Palmer. Residual lifetime and 10 year absolute risks of osteoporotic fractures in Chinese men and women. *CURR MED RES OPIN* 2015;31(6):1149-1156. doi: 10.1185/03007995.2015.1037729 pmid:258511772015-06-03].
4. B. Qu, Y. Ma, M. Yan, H. H. Wu, L. Fan, D. F. Liao, X. M. Pan, Z. Hong. The economic burden of fracture patients with osteoporosis in western China. *Osteoporos Int* 2014;25(7):1853-60. doi: 10.1007/s00198-014-2699-0 pmid:246916492014-07-01].
5. Tella SH, Gallagher JC. Prevention and treatment of postmenopausal osteoporosis. *J Steroid Biochem Mol Biol* 2014;142:155-70. <https://doi.org/10.1016/j.jsbmb.2013.09.008>.

6. G. F. Liu, Z. Q. Wang, L. Liu, B. T. Zhang, Y. Y. Miao, S. N. Yu. A network meta-analysis on the short-term efficacy and adverse events of different anti-osteoporosis drugs for the treatment of postmenopausal osteoporosis. *J CELL BIOCHEM* 2018;119(6):4469-4481. doi: 10.1002/jcb.26550 pmid:29227547. [(c) 2017 Wiley Periodicals, Inc.:*2018-06-01].
7. Lin J, Zhu J, Wang Y, Zhang N, Gober HJ, Qiu XM, Li DJ, Wang L. Chinese single herbs and active ingredients for postmenopausal osteoporosis: From preclinical evidence to action mechanism. *BIOSCI TRENDS* 2017;11(5):496-506. <https://doi.org/10.5582/bst.2017.01216>.
8. Zhang ND, Han T, Huang BK, Rahman K, Jiang YP, Xu HT, Qin LP, Xin HL, Zhang QY, Li YM. Traditional Chinese medicine formulas for the treatment of osteoporosis: Implication for antiosteoporotic medicine discovery. *J ETHNOPHARMACOL* 2016;189:61-80. <https://doi.org/10.1016/j.jep.2016.05.025>.
9. Chen MS, Zhang B, Zeng HB, Tang SD. Clinical study on treating postmenopausal osteoporosis of the ShenyinXu type with the Ziyin Tongluo prescription. *Clinical Journal of Chinese Medicine* 2019;11(14):108-110.2019-05-20.
10. Ru J, Li P, Wang J, Zhou W, Li B, Huang C, Li P, Guo Z, Tao W, Yang Y, Xu X, Li Y, Wang Y, Yang L. TCMSP: a database of systems pharmacology for medicine discovery from herbal medicines. *J Cheminform* 2014;6:13. <https://doi.org/10.1186/1758-2946-6-13>.
11. Liu Z, Guo F, Wang Y, Li C, Zhang X, Li H, Diao L, Gu J, Wang W, Li D, He F. BATMAN-TCM: a Bioinformatics Analysis Tool for Molecular mechANism of Traditional Chinese Medicine. *Sci Rep.* 2016, 6:21146. <https://doi.org/10.1038/srep21146>.
12. Lin Huang, Duoli Xie, Yiran Yu, Huanlong Liu, Yan Shi, Tieliu Shi, Chengping Wen. TCMID 2.0: a comprehensive resource for TCM. *NUCLEIC ACIDS RES* 2018;46(D1):D1117-D1120. <https://doi.org/doi:10.1093/nar/gkx1028>.
13. UniProt: a worldwide hub of protein knowledge. *NUCLEIC ACIDS RES* 2019;47(D1):D506-D515. <https://doi.org/10.1093/nar/gky1049>.
14. Safran M. Human Gene-Centric Databases at the Weizmann Institute of Science: GeneCards, UDB, CroW 21 and HORDE. *NUCLEIC ACIDS RES* 2003;31(1):142-146. <https://doi.org/10.1093/nar/gkg050>.
15. Amberger JS, Hamosh A. Searching Online Mendelian Inheritance in Man (OMIM): A Knowledgebase of Human Genes and Genetic Phenotypes. *Current Protocols in Bioinformatics* 2017;58(1). <https://doi.org/10.1002/cpbi.27>.
16. Janet Piñero, Juan Manuel Ramírez-Anguita, Josep Saüch-Pitarch, Francesco Ronzano, Emilio Centeno, Ferran Sanz, Laura I. Furlong. The DisGeNET knowledge platform for disease genomics: 2019 update. *NUCLEIC ACIDS RES* 2019. <https://doi.org/10.1093/nar/gkz1021>.
17. Doncheva NT, Morris JH, Gorodkin J, Jensen LJ. Cytoscape StringApp: Network Analysis and Visualization of Proteomics Data. *J PROTEOME RES* 2018;18(2):623-632. <https://doi.org/doi:10.1021/acs.jproteome.8b00702>.
18. Tang Y, Li M, Wang JX, Pan Y, Wu FX. CytoNCA: A cytoscape plugin for centrality analysis and evaluation of protein interaction networks. *BIOSYSTEMS* 2015;127:67-72. <https://doi.org/doi:10.1021/acs.jproteome.8b00702>.
19. Szklarczyk D, Gable AL, Lyon D, Junge A, Wyder S, Huerta-Cepas J, Simonovic M, Doncheva NT, Morris JH, Bork P, Jensen LJ, Mering CV. STRING v11: protein-protein association networks with increased coverage, supporting functional discovery in genome-wide experimental datasets. *NUCLEIC ACIDS RES* 2019;47(D1):D607-D613. <https://doi.org/10.1093/nar/gky1131>.
20. Huang DW, Sherman BT, Lempicki RA. Systematic and integrative analysis of large gene lists using DAVID bioinformatics resources. *NAT PROTOC* 2009;4(1):44-57. <https://doi.org/10.1038/nprot.2008.211>.
21. Huang DW, Sherman BT, Lempicki RA. Bioinformatics enrichment tools: paths toward the comprehensive functional analysis of large gene lists. *NUCLEIC ACIDS RES* 2009;37(1):1-13. <https://doi.org/10.1093/nar/gkn923>.
22. Zheng JH, Wu M, Wang HY, Li SS, Wang X, Li Y, Wang D, Li S. Network Pharmacology to Unveil the Biological Basis of Health-Strengthening Herbal Medicine in Cancer Treatment. *CANCERS* 2018;10(11):461. <https://doi.org/10.3390/cancers10110461>
23. Ranganathan Babujanathanam, Purushothaman Kavitha, U. S. Mahadeva Rao, Moses Rajasekara Pandian. Quercitrin a bioflavonoid improves the antioxidant status in streptozotocin: induced diabetic rat tissues. *MOL CELL BIOCHEM* 2011;358(1-2):121-129. <https://doi.org/10.1007/s11010-011-0927-x>.
24. Ward AB, Mir H, Kapur N, Gales DN, Carriere PP, Singh S. Quercetin inhibits prostate cancer by attenuating cell survival and inhibiting anti-apoptotic pathways. *WORLD J SURG ONCOL* 2018;16(1). <https://doi.org/10.1186/s12957-018-1400-z>.
25. Cruz EA, Da-Silva SAG, Muzitano M F, Silva PM R, Costa SS, Rossi-Bergmann B. Immunomodulatory pretreatment with *Kalanchoe pinnata* extract and its quercitrin flavonoid effectively protects mice against fatal anaphylactic shock. *INT IMMUNOPHARMACOL* 2008;8(12):1616-1621. <https://doi.org/10.1016/j.intimp.2008.07.006>.
26. Kim JA, Jung YS, Kim MY, Yang SY, Lee S, Kim YH. Protective Effect of Components Isolated from *Lindera erythrocarpa* against Oxidative Stress-induced Apoptosis of H9c2 Cardiomyocytes. *PHYTOTHER RES* 2011;25(11):1612-1617. <https://doi.org/10.1002/ptr.3465>.
27. Xing LZ, Ni HJ, Wang YL. Quercitrin attenuates osteoporosis in ovariectomized rats by regulating mitogen-activated protein kinase (MAPK) signaling pathways. *BIOMED PHARMACOTHER* 2017;89:1136-1141. <https://doi.org/10.1016/j.biopha.2017.02.073>.

28. Nowak B, Matuszewska A, Nikodem A, Filipiak J, Landwójtowicz M, Sadanowicz E, Jędrzejuk D, Rzeszutko M, Zduniak K, Piasecki T, Kowalski P, Dziewiszek W, Merwid-Łąd A, Trocha M, Sozański T, Kwiatkowska J, Bolanowski M, Szelaż A. Oral administration of kaempferol inhibits bone loss in rat model of ovariectomy-induced osteopenia. *PHARMACOL REP* 2017;69(5):1113-1119. [https://doi.org/ 10.1016/j.pharep.2017.05.002](https://doi.org/10.1016/j.pharep.2017.05.002).
29. Wong SK, Chin KY, Ima-Nirwana S. The Osteoprotective Effects Of Kaempferol: The Evidence From In Vivo And In Vitro Studies. 2019;Volume 13:3497-3514. [https://doi.org/ 10.2147/DDDT.S227738](https://doi.org/10.2147/DDDT.S227738).
30. Melville KM, Kelly NH, Khan SA, Schimenti JC, Ross FP, Main RP, Meulen MCH. Female Mice Lacking Estrogen Receptor-Alpha in Osteoblasts Have Compromised Bone Mass and Strength. *J BONE MINER RES* 2014;29(2):370-379. <https://doi.org/10.1002/jbmr.2082>.
31. Wong SK, Chin KY, Ima-Nirwana S. The Osteoprotective Effects Of Kaempferol: The Evidence From In Vivo And In Vitro Studies. 2019;Volume 13:3497-3514. [https://doi.org/ 10.2147/DDDT.S227738](https://doi.org/10.2147/DDDT.S227738).
32. Zha L, He L, Liang YJ, Qin H, Yu B, Chang LL, Xue L. TNF- α contributes to postmenopausal osteoporosis by synergistically promoting RANKL-induced osteoclast formation. *BIOMED PHARMACOTHER* 2018;102:369-374. <https://doi.org/10.1016/j.biopha.2018.03.080>.
33. A. Shoukry, S. M. Shalaby, R. L. Etewa, H. S. Ahmed, H. M. Abdelrahman. Association of estrogen receptor beta and estrogen-related receptor alpha gene polymorphisms with bone mineral density in postmenopausal women. *MOL CELL BIOCHEM* 2015;405(1-2):23-31. doi: 10.1007/s11010-015-2391-5 [pmid:259034002015-07-01].
34. Moriarty K, Kim KH, Bender JR. Estrogen Receptor-Mediated Rapid Signaling. *ENDOCRINOLOGY* 2006;147(12):5557-5563. <https://doi.org/10.1210/en.2006-0729>.
35. Sharma AR, Nam JS. Kaempferol stimulates WNT/ β -catenin signaling pathway to induce differentiation of osteoblasts. *J Nutri Biochem* 2019;74:108228. <https://doi.org/10.1016/j.jnutbio.2019.108228>.

| Pharmaceutical name | Botanical or zoological name | Chinese | Content |
|---------------------------------------|-------------------------------------|---------------|---------|
| Radix Rehmanniae Praeparatae | Rehmannia glutinosa Libosch | Shu Di | 10g |
| Ophiopogon japonicus | Ophiopogonis Japonicum Tuber | Mai Dong | 10g |
| Achyranthes bidentata | Achyranthes Bidentata Radix | Niu Xi | 10g |
| Fructus Ligustri Lucidi | Ligustrum lucidum Ait [fruit] | Nv Zhen Zi | 10g |
| Radix Angelicae Sinensis | Angelica sinensis (Oliv.) Diels | Dang Gui | 10g |
| Radix Paeoniae Alba | Paeonia lactiflora Pall | Bai Shao | 10g |
| Loranthus parasiticus | Viscum Coloratum seu Loranthi Ramus | Sang Ji sheng | 15g |
| Radix Astragali | Astragalus mongholicus | Huang Qi | 10g |
| Zaocys | Ptyas dhumnades | Wu Shao She | 10g |
| Caulis Spatholobi | Spatholobus suberectus Dunn | Ji Xue Teng | 15g |
| Scolopendra | Scolopendra subspinipes mutilans | Wu Gong | 10g |
| Saposhnikoviae Radix | Ledebouriella Sesloides Radix | Fang Feng | 10g |
| Rhizoma Atractylodis Macrocephalae | Atractylodes macrocephala Koidz | Bai Zhu | 10g |
| Radix Glycyrrhizae Preparata | Glycyrrhiza uralensis Fisch | Gan Cao | 3g |

Table1 Composition of ZYTLF

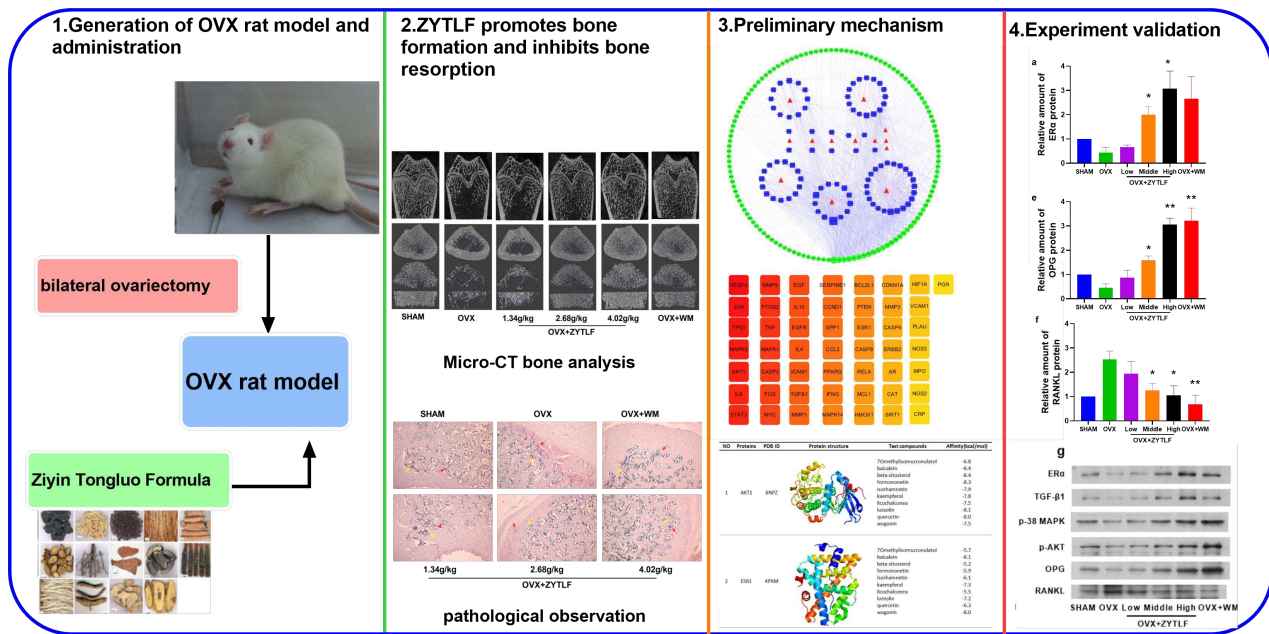


Figure1 Flowchart of the work

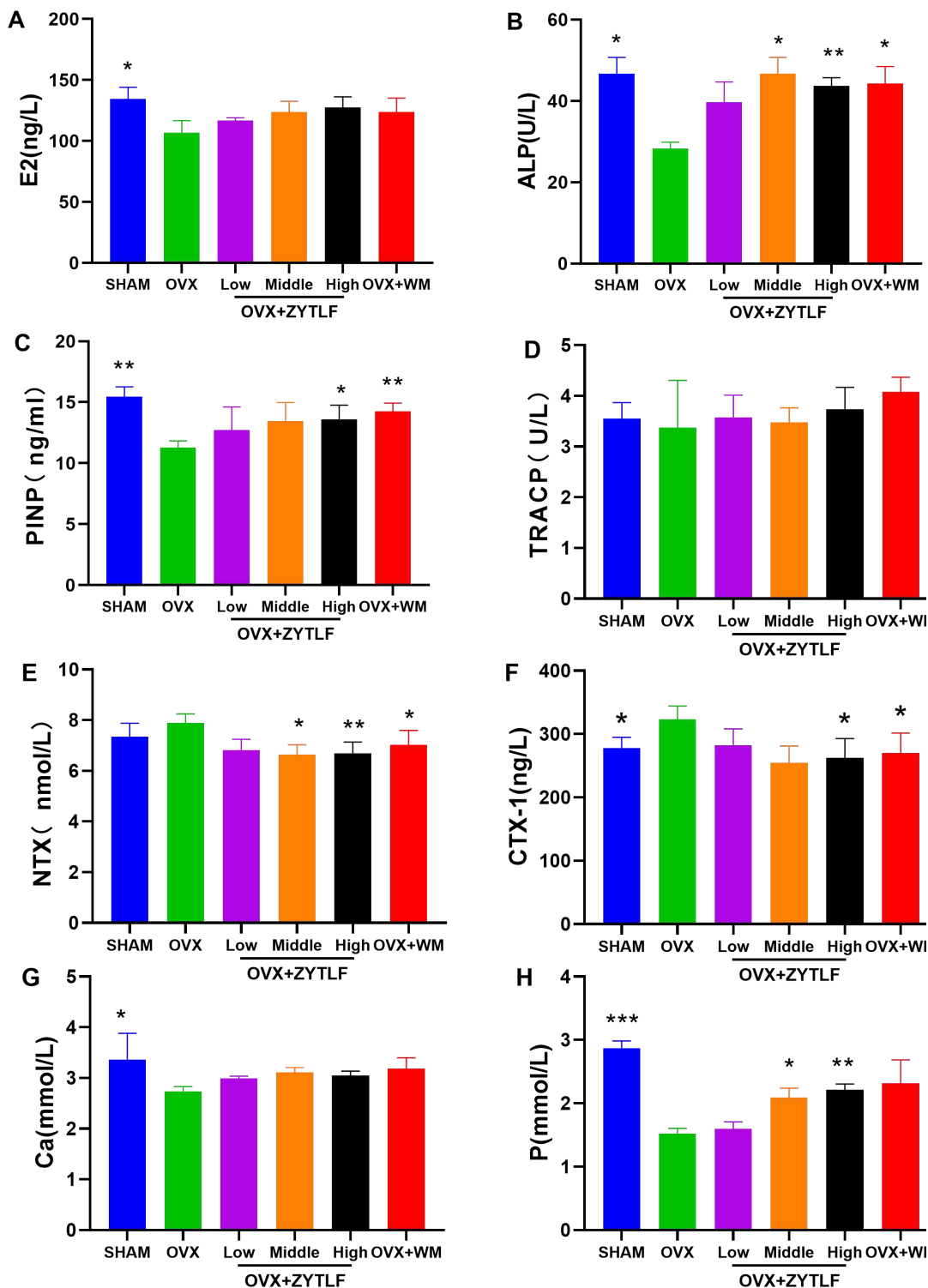


Figure 2 Effects of ZYTLF on serum indicators in OVX rat.

a estradiol (E2) **b** alkaline phosphatase (ALP) **c** procollagen I N-terminal propeptide (PINP) **d** tartrate-resistant acid phosphatase (TRACP) **e** type I collagen cross-linked Amino Terminal Peptide (NTX) **f** type I collagen cross-linked carboxyl Terminal Peptide (CTX-1) **g** calcium (Ca) **h** phosphorus (P). The results were shown as the mean \pm SD (n=9 rats per group). Low:1.34g/kg; Middle:2.68g/kg; High:4.02g/kg; Western Medicine: alendronate 10.51mg/kg per week and calcitriol 0.075 μ g/kg per day. *p<0.05, **p<0.01, when compared with OVX group.

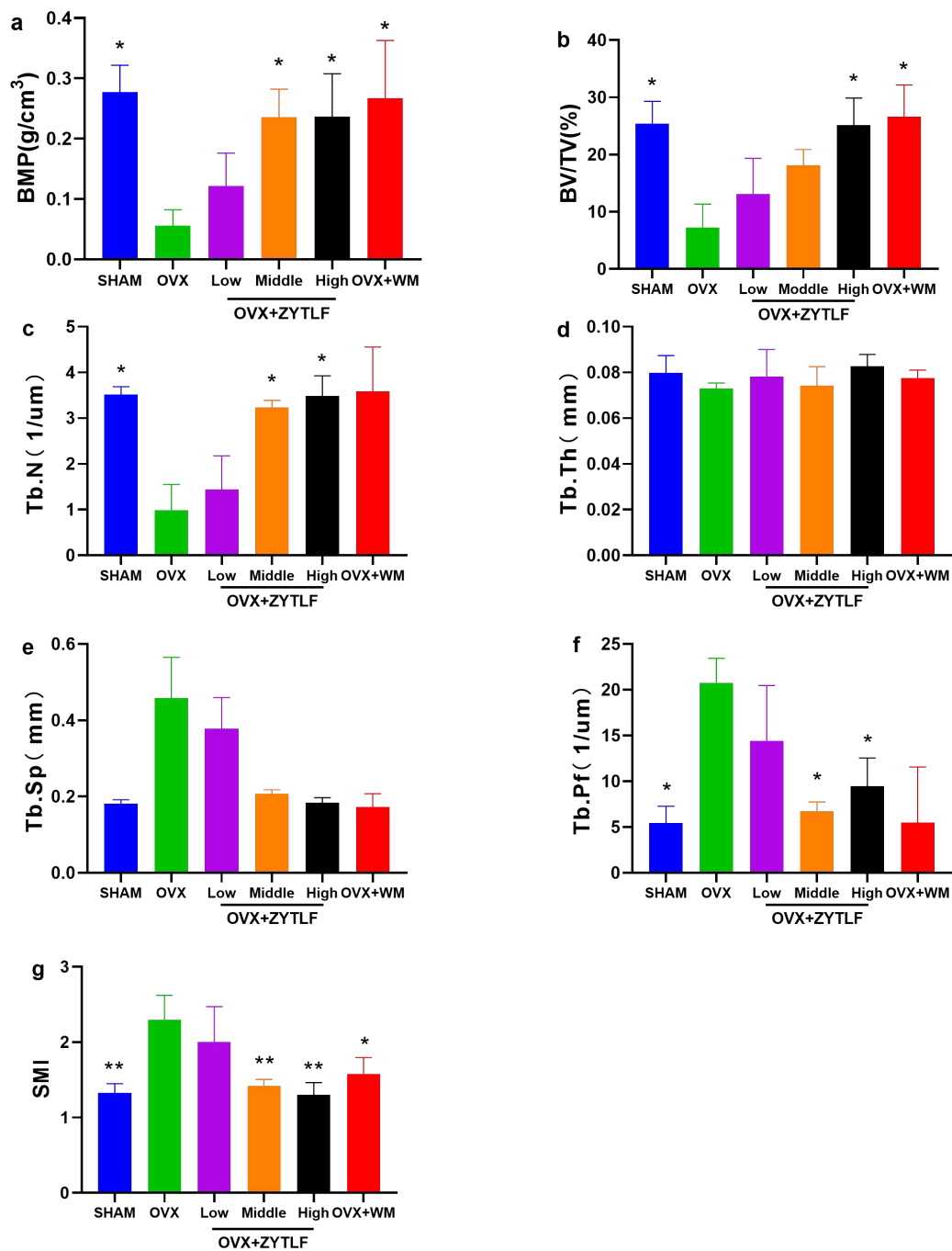


Figure3 The effect of ZYTLF on trabecular bone parameters in the right distal femur of OVX rats.

Parameters assessed: **a** bone mineral density (BMD). **b** bone volume fraction (BV/TV). **c** trabecular number (Tb.N). **d** trabecular thickness (Tb.Th). **e** trabecular separation (Tb.Sp). **f** trabecular bone pattern factor (Tb.Pf). **g** structure model index (SMI).

The results were shown as the mean \pm SD. Low:1.34g/kg; Middle:2.68g/kg; High:4.02g/kg; Western Medicine: alendronate 10.51mg/kg per week and calcitriol 0.075 μ g/kg per day. * P<0.05, ** P<0.01 compared with OVX group.

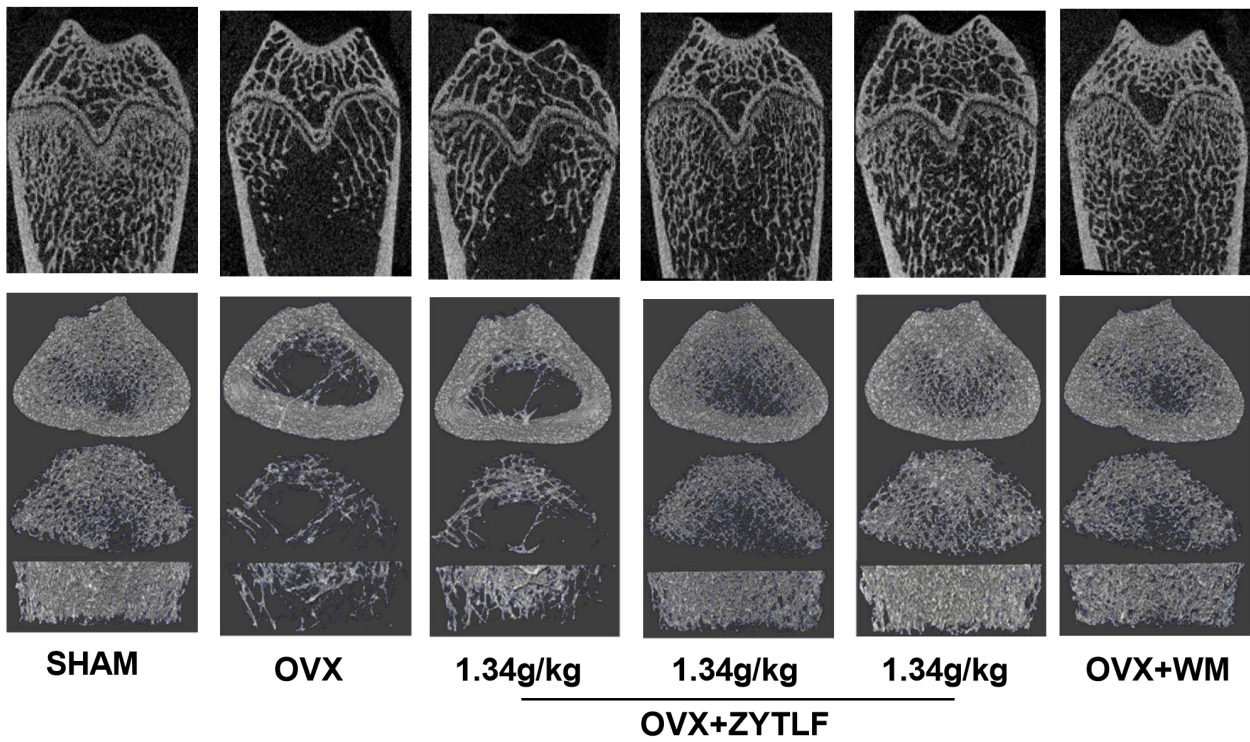


Figure4 Micro-CT scan of the right distal femur

Representative plain scan images of the distal femur were shown (sagittal and transverse) in SHAM, OVX, OVX+ZYTLF (1.34g/kg), OVX+ZYTLF(2.68g/kg), OVX+ZYTLF(4.02g/kg) , OVX+WM (Western Medicine) respectively.

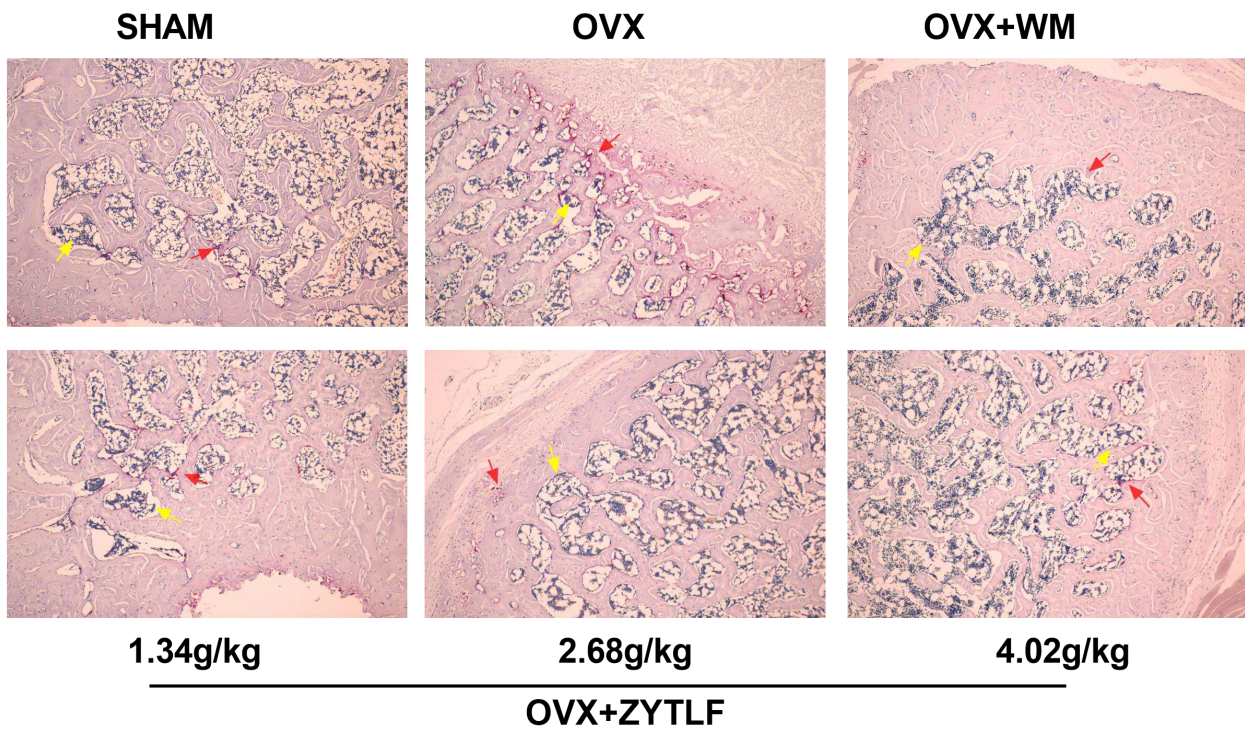


Figure5 ZYTFLF inhibited the formation of osteoclast in OVX rats.

After treating, ALP+TRACP staining were performed and the results were shown in above (10X). The cytoplasm of osteoclasts is wine-red and the cytoplasm of osteoblasts shows grayish-black granules, noted by red and yellow arrow respectively.

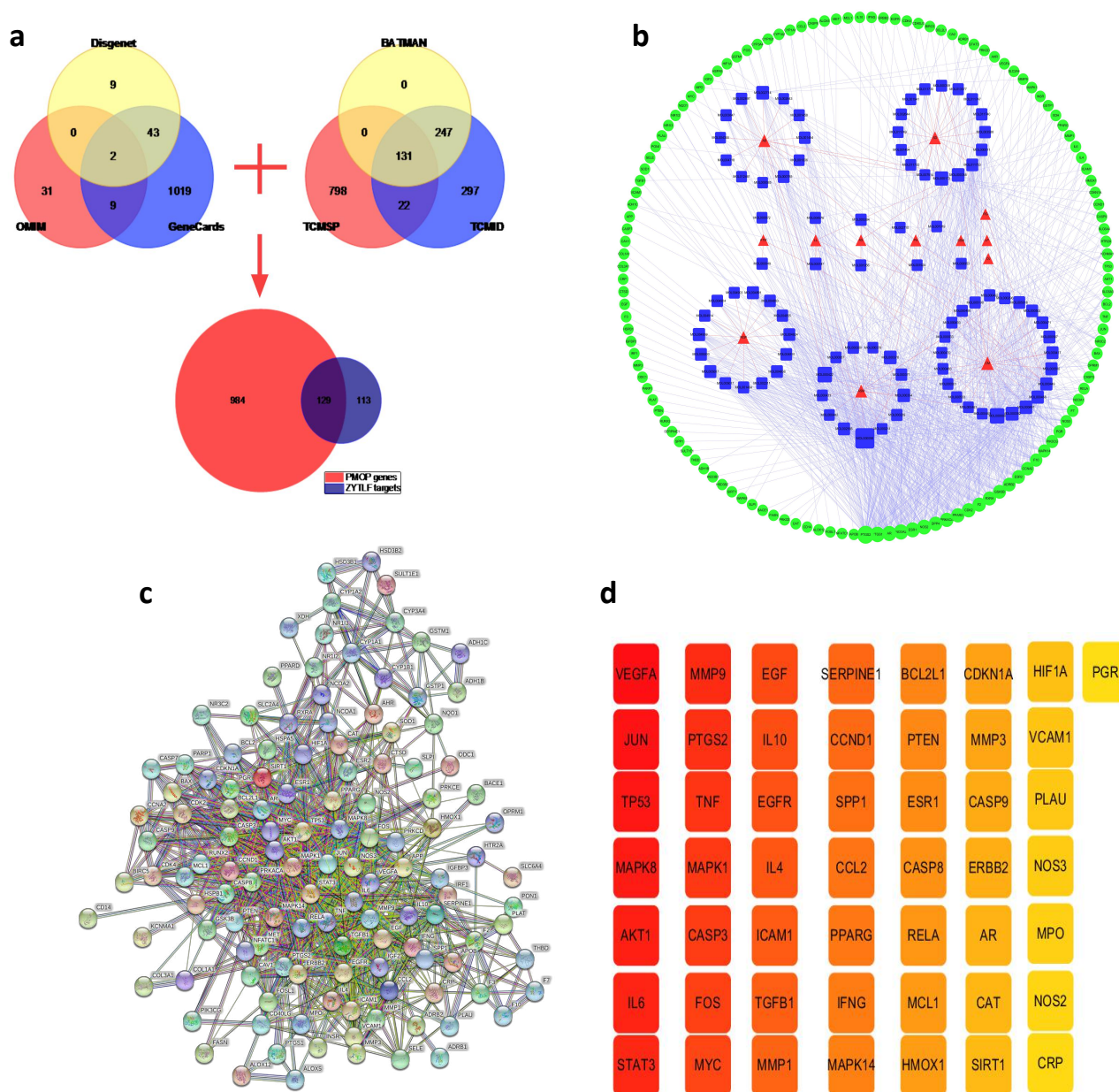


Figure6 Hub proteins of ZYTLF were determined by network pharmacology technology

a Venn diagram: 129 overlapping genes were selected as potential targets for further study. **b** The

herb-compound-overlapping gene" network: the red triangle represent traditional Chinese herbs of ZYTLF, blue square represent compounds, and green circle represent overlapping target genes. Lines represent relationship between nodes.

And the larger of nodes, the higher degree of constituent. **c** Protein-protein interaction (PPI) network of 129 overlapping

proteins. **d** 50 hub proteins: after computing the overlapping proteins, hub proteins were screened. The color of the node

changed from light yellow to dark red, indicating that the higher the MCC value was, the more significant the role it played in the network.

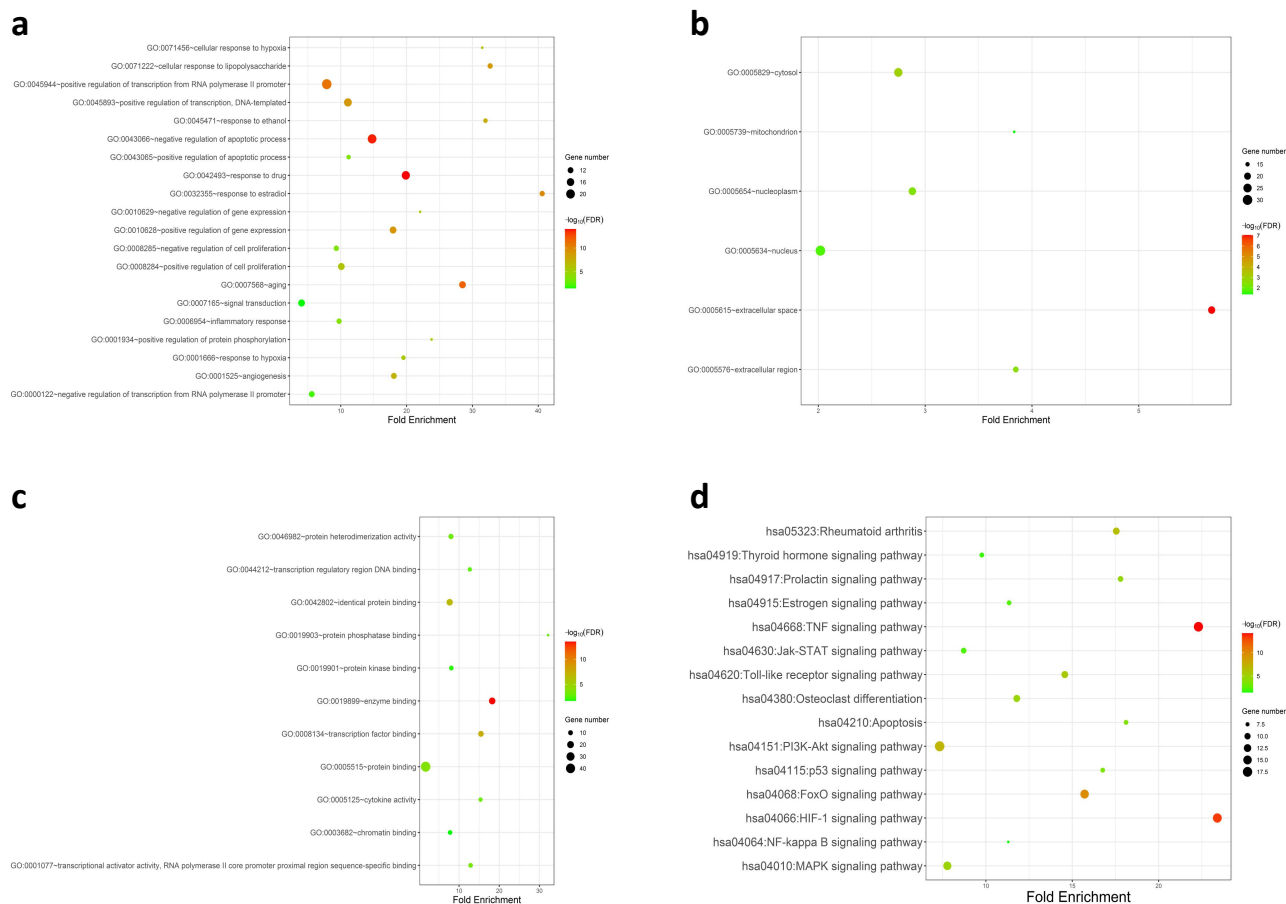
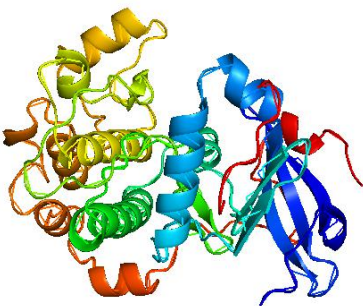
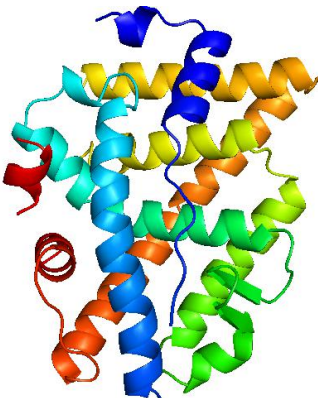
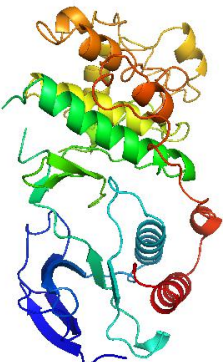
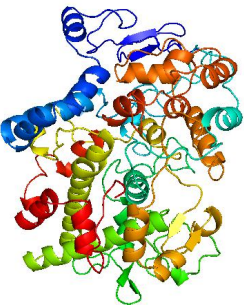
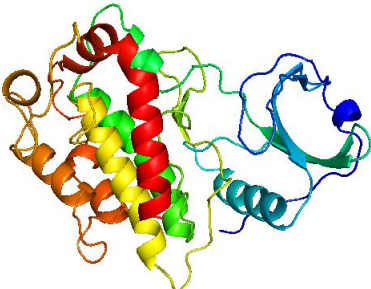


Figure 7 GO analysis and KEGG pathway enrichment analysis of Key gene

In the bubble diagrams above (a-d), the ordinate represents the names of BP, CC, MF terms and pathways, respectively, and the abscissa represents the degree of enrichment. The smaller the FDR is, the higher the importance of enrichment, and the redder the color on the diagram.

| | | | | | |
|---|---------------|------|-------------------------------------------------------------------------------------|-------------------------------------------------------------------------------------------------------------------------------------------------------------|------------------------------------------------------------------------------|
| 1 | AKT1 | 6NPZ |  | 7Omethyilisomucronulatol baicalein beta-sitosterol formononetin isorhamnetin kaempferol licochalconea luteolin quercetin wogonin | -6.8 -8.4 -8.4 -8.3 -7.9 -7.8 -7.5 -8.1 -8.0 -7.5 |
| 2 | ESR1 | 4PXM |  | 7Omethyilisomucronulatol baicalein beta-sitosterol formononetin isorhamnetin kaempferol licochalconea luteolin quercetin wogonin | -5.7 -8.1 -5.2 -5.9 -6.1 -7.3 -5.5 -7.2 -6.3 -8.0 |
| 3 | MAPK14 | 6SFO |  | 7Omethyilisomucronulatol baicalein beta-sitosterol formononetin isorhamnetin kaempferol licochalconea luteolin quercetin wogonin | -7.4 -9.6 -7.4 -9.3 -8.7 -9.2 -8.3 -9.3 -9.3 -8.9 |
| 4 | PTGS2 | 5F19 |  | 7Omethyilisomucronulatol baicalein beta-sitosterol formononetin isorhamnetin kaempferol licochalconea luteolin quercetin wogonin | -7.5 -9.0 -7.3 -8.4 -9.2 -8.1 -8.9 -8.9 -8.7 -8.4 |
| 5 | TNF- α | 3M2W |  | 7Omethyilisomucronulatol baicalein beta-sitosterol formononetin isorhamnetin kaempferol licochalconea luteolin quercetin wogonin | -7.7 -9.4 -9.2 -9.0 -9.1 -8.9 -8.7 -9.5 -9.2 -9.2 |

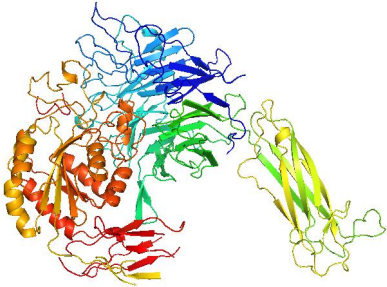
| | | | | | |
|---|---------------|------|-----------------------------------------------------------------------------------|--------------------------|------|
| 6 | TGF β 1 | 5VQP |  | 7Omethyloisomucronulatol | -8.3 |
| | | | | baicalein | -7.6 |
| | | | | beta-sitosterol | -7.9 |
| | | | | formononetin | -9.3 |
| | | | | isorhamnetin | -8.5 |
| | | | | kaempferol | -8.4 |
| | | | | litchalconea | -9.0 |
| | | | | luteolin | -7.3 |
| | | | | quercetin | -9.4 |
| | | | | wogonin | -8.5 |

Table2 Information of key proteins and compounds by molecular docking

When the binding energy is less than -5 kcal/mol, the ligands and receptors are considered to be able to form stable compounds.

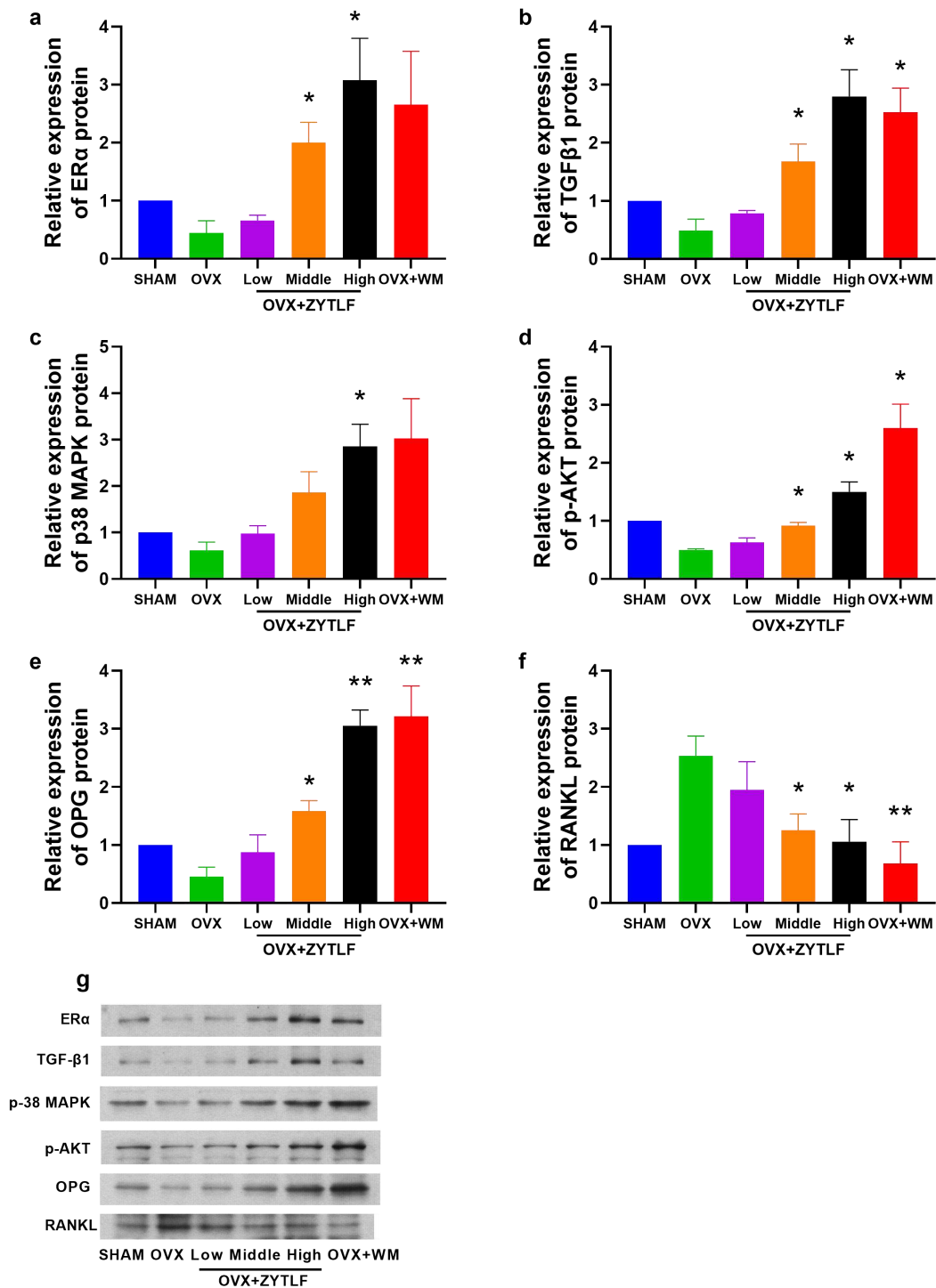


Figure 8 Effects of ZYTLF on expressions of key proteins

After treatment, the relative expression of ER α (a), p38 MAPK (b), p-AKT (c), TGF- β 1(d), OPG (e), RANKL(f) and the western blots of key proteins (G) in bone were shown.

The results were shown as the mean \pm SD. Low:1.34g/kg; Middle:2.68g/kg; High:4.02g/kg; Western Medicine: alendronate 10.51mg/kg per week and calcitriol 0.075 μ g/kg per day. * P<0.05, ** P<0.01 compared with OVX group.

Supplementary Files

This is a list of supplementary files associated with this preprint. Click to download.

- [Additionalfile1TableS1.xls](#)
- [Additionalfile2TableS2.xls](#)
- [Additionalfile3TableS3.xls](#)
- [Additionalfile4TableS4.xls](#)
- [Additionalfile5TableS5.xls](#)
- [PointtoPointresponsetoreviews.docx](#)